A critical review on free edge delamination fracture criteria

Mohammad Burhan[1], Zahur Ullah[1,2 *], Zafer Kazancı[1], Giuseppe Catalanotti[1,3 †]

[1] Advanced Composites Research Group, School of Mechanical and Aerospace Engineering, Queen's University Belfast, Ashby Building, Belfast. Northern Ireland, BT9 5AH, UK.

[2] Durham University, South Road, Durham, DH1 3LE, UK

[3] Dipartimento di Ingegneria e Architettura, Università degli Studi di Enna Kore, Cittadella Universitaria, Enna, 94100, Italy. Department of Engineering.

Abstract

Laminates experience three-dimensional singular stress near their free edges due to elastic mismatches between layers, which can cause delamination. This paper critically evaluates methods for predicting free edge delamination and highlights the limitations of conventional strength-of-materials and fracture mechanics approaches. The Theory of Critical Distances (TCD) uses a material-dependent critical distance parameter, while Finite Fracture Mechanics (FFM) employs a combined stress-energy criterion without needing a predefined length parameter. This review compares TCD and FFM, also discussing Cohesive Zone Models and Phase-Field Models, and aims to guide the selection of appropriate methods for analysing free edge delamination.

Keywords:

Energy release rate (ERR), Interlaminar stresses, Free edge effect, Delamination, Composite laminates.

*Corresponding Author (Zahur Ullah): zahur.ullah@durham.ac.uk

†Corresponding Author (Giuseppe Catalanotti): giuseppe.catalanotti@unikore.it

Nomenclature

c_o	Critical distance in Point Method
d_o	Critical distance in Line Method
d	Damage Variable
E_{LAM}	Axial stiffness (tangent modulus) of symmetric uncracked laminate
E_i	Axial stiffness of i^{th} sublaminate
E^*	Axial stiffness of completely delaminated laminate

G_c	Fracture toughness
G	Energy release rate
$I/II/III$	Different modes of fracture
k_c	Critical stress intensity factor
k	Stress intensity factor
K	Penalty stiffness
n	Normalised effective ply thickness
S	Strength
S_x, S_y	Interlaminar shear strengths for σ_{xz}, σ_{yz}, σ_{zz}
S_z	Interlaminar normal tensile strength for σ_{zz}
S_z^c	Interlaminar normal compressive strength for σ_{zz}
t	Laminate thickness
t_i	Thickness of i^{th} sublaminate
x, y, z	Global coordinate system
δ	Remote tensile displacement
Δ	Separation
Δa	Finite crack extension
ΔT_f	Critical thermal load
Δ^o	Damage onset separation
Δ^f	Critical opening
ε	Nominal strain
ε_c	Delamination onset strain
θ	Ply orientation
σ	Stress
σ_{xy}	In-plane shear stress
σ_{yy}	Transverse normal stress
σ_{iz}	Interlaminar stress component
$\overline{\sigma}_{iz}$	Average interlaminar stress component
τ	Traction between the potential crack surfaces
τ^o	Material strength
CLPT	Classical Laminate Plate Theory

CZM	Cohesive Zone Models
ERR	Energy Release Rate
FCE	Finite Crack Extension
FEA	Finite Element Analysis
FEM	Finite Element Method
FFM	Finite Facture Mechanics
ICM	Imaginary Crack Method
LEFM	Linear Elastic Fracture Mechanics
LM	Line Method
PFM	Phase-Field Models
PM	Point Method
SIF	Stress Intensity Factor
TCD	Theory of Critical Distances

1. Introduction

In recent years, lightweight engineering has emerged as a pivotal technology essential for achieving high energy efficiency and enhanced fuel economy across all industries, aligning with the global vision of attaining climate neutrality by 2050 [1]. As a lightweight material, fibre-reinforced polymer composites due to possessing exceptional properties, including superior fatigue life, outstanding corrosive resistance, high specific strength, and stiffness, have been widely utilised in aerospace, marine, automobile, and construction industries [2–5]. However, despite numerous benefits and advantages, composite laminates are susceptible to complex failure modes, with delamination standing out as the most concerning one. Interlaminar stresses that arise in the vicinity of various material and/or geometric discontinuities, as depicted in Fig. 1, are highly localised with steep gradients and therefore may lead to delamination.

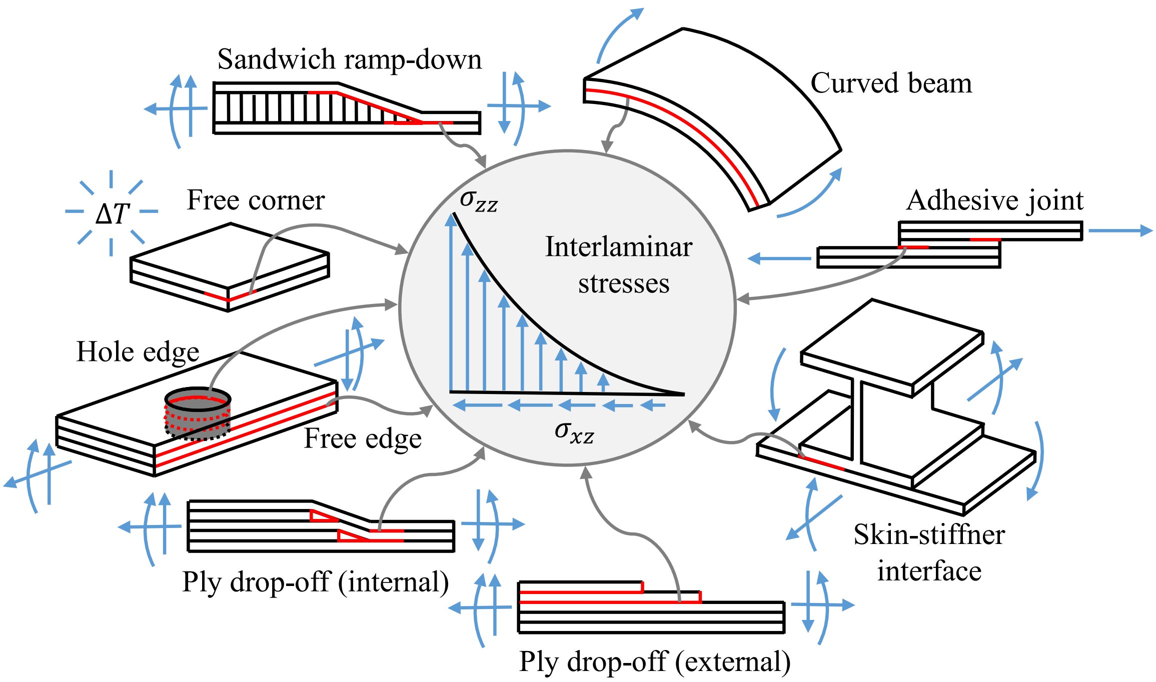

Fig. 1. Interlaminar stresses that arise from different material and geometric discontinuities.

1.1. Background

One prominent example of singular interlaminar stresses that emerge due to a mismatch in elastic properties of the individual plies is the so-called free edge effect. To clarify the singular nature of interlaminar stresses at the free edge of the laminate, a symmetric four-layer laminate, as illustrated in Fig. 2, is considered. Since Composite Laminate Plate Theory (CLPT) is two-dimensional, it is unable to capture interlaminar stresses. Shear deformation theories, such as

[6], and layerwise theories, such as [7], provide significant improvements over CLPT in addressing these limitations. Although the occurrences of interlaminar stresses near the free edge can be readily explained through the scenarios illustrated in Fig. 3 for cross-ply and Fig. 4 for angle-ply laminates. Moreover, it is noted that their occurrences in a laminate with a general layup can be explained in the same way as those in cross-ply or angle-ply laminates.

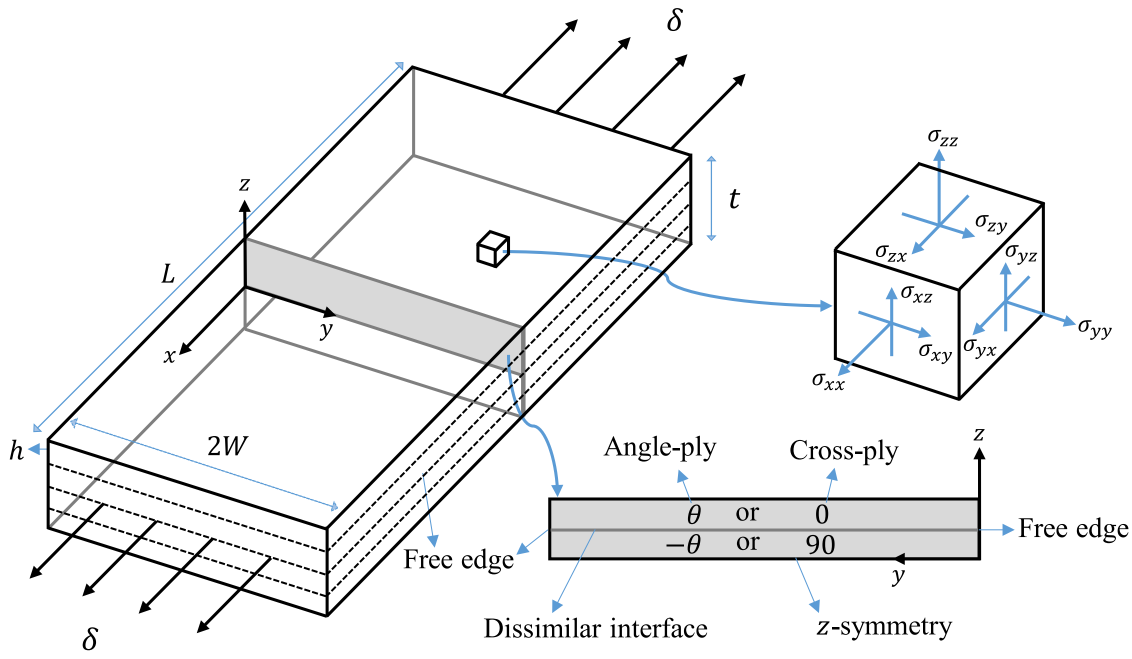

Fig. 2. A schematic diagram of a four-layer symmetric laminate with free edge.

In the case of unbounded 0° and 90° layers in a cross-ply $[0/90]_s$ laminate (Fig. 3), the difference in Poisson's ratios results in different transverse deformations when subjected to uniform remote tensile displacement δ. When bonded together, displacement compatibility at the interface of 0° and 90° layers induce interlaminar shear stress σ_{yz}. This σ_{yz} tends to expand 0° layer and contract 90° layer laterally. The accompanying free body diagram in the figure shows the development of interlaminar stresses at the 0/90 interface, including a normal stress σ_{yy} in the y-direction. While σ_{yy} balances the transverse forces with σ_{yz}, a moment is generated in the yz-plane due to their different lines of action. This moment is equilibrated by the moment induced by interlaminar normal stress σ_{zz}, which exerts no net force in the through-the-thickness z-direction but exhibits a mathematical singularity at the free edge, making the interface prone to delamination. The distribution of interlaminar stresses at the 0/90 interface is illustrated in the bottom right of the same figure.

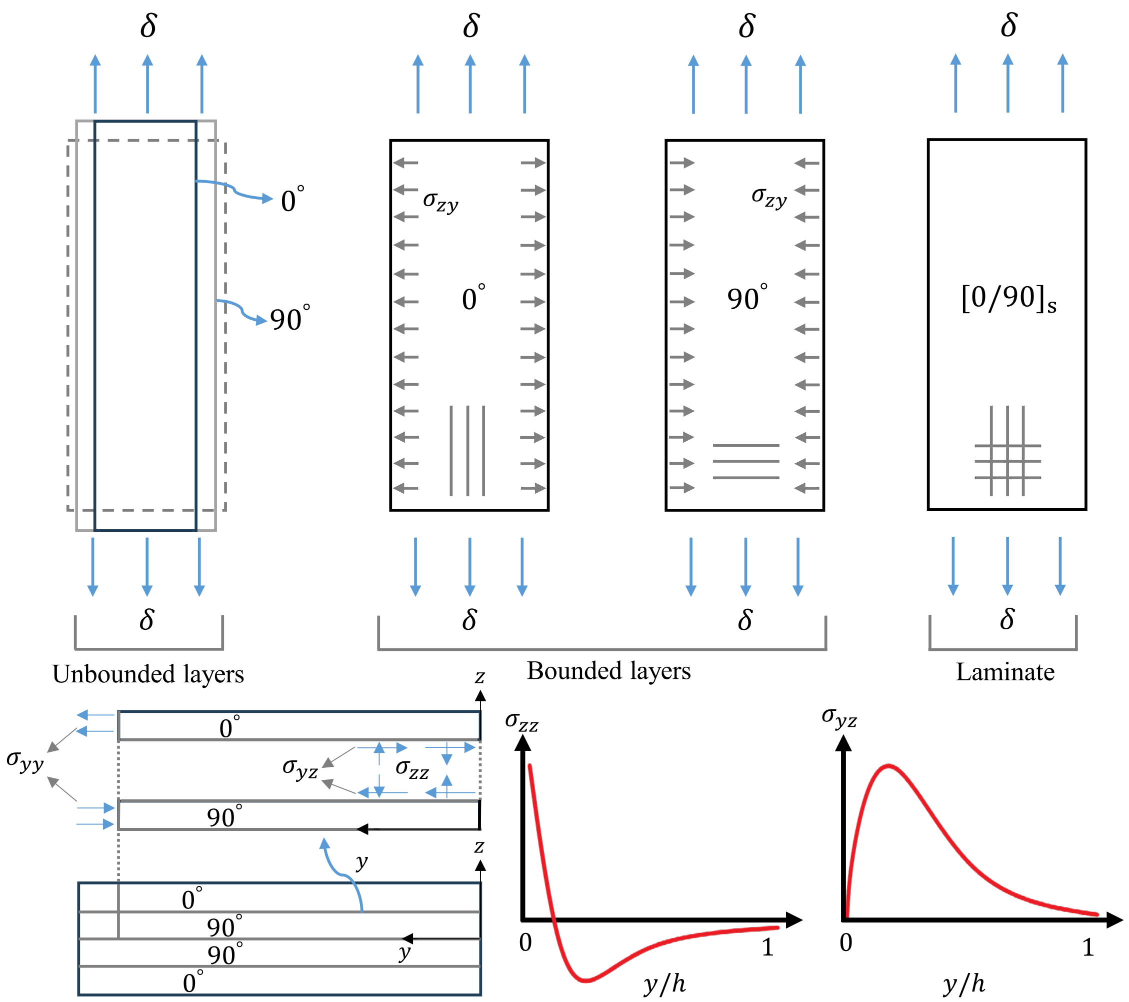

Fig. 3. The free edge effect in cross-ply laminate.

At the dissimilar $\theta/-\theta$ interface in angle ply laminate $[\pm\theta]_s$, different state of interlaminar stresses manifest. When subjected to uniform remote tensile displacement δ and considered unbounded (see Fig. 4), the layers undergo in-plane shear deformation. Upon bounded together, the compatibility of resultant displacement induces the interlaminar shear stress σ_{xz} at the $\theta/-\theta$ interface. This σ_{xz} is balanced by in-plane shear σ_{xy} in the longitudinal x-direction of the laminate, as shown in the free body diagram. Notably, a mathematical singularity in the distribution of σ_{xz} occurs at the free edge of the dissimilar $\theta/-\theta$ interface, as depicted in the bottom right of the same figure, making angle-ply laminates susceptible to delamination.

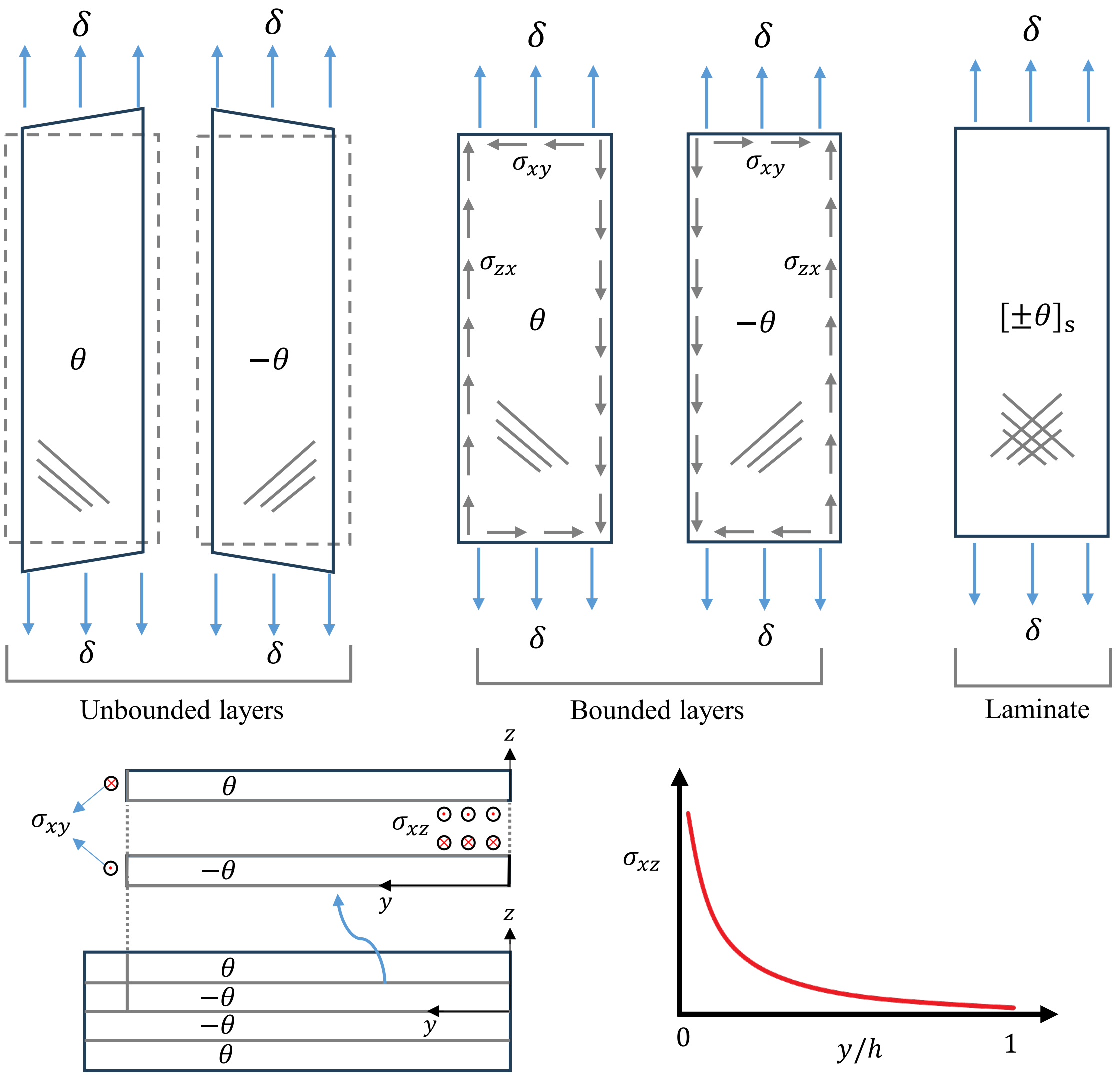

Fig. 4. The free edge effect in angle-ply laminate.

Since the interlaminar stresses may lead to free edge delamination, it has attained a high practical significance and attention from the scientific community. Since Hayashi's [8] first description of the free edge effect in the late 1960s, the topic has been extensively studied. Despite this, no exact solution exists for the elasticity equations governing the free edge effect [9] due to the intrinsic complexities associated with the problem. As a result, various approaches have been presented to address this effect. Pagano and Pipes [10,11] as well as Kassapoglou and Lagace [12], utilised approximate closed-form techniques to study interlaminar stresses at free edges. Meanwhile, Wang and Choi [13,14] analysed the stress singularities order through an analytical approach. Recent closed-form analytical techniques [15,16] have utilised an inner solution approach based on CLPT and mathematical layers, acquired from the discretization of physical plies for the prediction of free edge effects. Studies [17–19] employed a layer-wise laminated theory and the improved first-order shear deformation theory (IFSDT) for calculating interlaminar stresses. Tahani and Nosier [20] analytically investigated interlaminar stresses in cross-ply symmetric and unsymmetric laminates under mechanical and hygrothermal loadings with various boundary conditions using layerwise theory. According to Carrera's Unified Formulation (CUF) [21], Wenzel et al. [22] employed CUF plate elements for identifying stress singularity at the free edge and assessed symmetric laminates for free edge effect under extension and bending. In contrast, some researchers adopted numerical methods, including the finite difference approach [23], a quasi-2D plane strain model within the finite element method (FEM) framework [24], a 3D FEM [25,26] for examining stress singularities at free edges, and a boundary layer approach [27].

There are other structural configurations closely related to the free edge effect that give rise to interlaminar stresses; however, the focus here is on a selection of key studies. Ahmadi [28] utilised and formulated the displacement-based layerwise laminate theory to investigate the interlaminar stresses at the free edge of a thick composite cylinder with general stacking of layers under uniform and non-uniform internal and external pressure. While Wang et al. [29] obtained elasticity solution of interlaminar stresses in a cylindrical shell stacked as a cross-ply under radial pressure by employing orthotopic elastic theory. Kappel et al. [30] introduced semi-analytical approaches for the free edge stresses in cross-ply cylindrical laminated shells under hygrothermomechanical loading conditions. Additionally, Shim and Lagacé [31] presented an analytical method for the determination of interlaminar stresses in laminates with ply drop-offs. By using the elastic-plastic finite element method, Ding et al. [32] investigated the interlaminar stresses along the hole edge at different interfaces of thick composite laminates under tension. A closed-form method for the determination of interlaminar stresses in the vicinity of reinforcement patch corner, rectangular in shape, of a cross-ply laminate subjected to thermal loading is presented by Wigger and Becker [33]. Motivated by the works of Ivanova et al. [34] in designing the bi-material piezoelectric laminate, Wu and Han [35] employed the state space approach in generalised plane strain piezoelasticity for the investigation of free edge effect.

Furthermore, several review papers have covered this subject extensively (see Refs. [36–38]). A recent comprehensive review detailing developments in this area over the past two decades can be found in Ref. [9].

1.2. Problem statement, motivation, and scope of the paper

The interlaminar fracture due to free edges can be induced under various loading conditions, including quasi-static, fatigue, thermal, or moisture exposure. This concern extends not only to monolithic composite laminates but also to hybrid metal/composite laminates [39]. To address delamination caused by interlaminar stresses, it is essential to use a suitable fracture criterion for crack initiation prediction at singular stress raisers, such as free edges.

Given the presence of singular stresses at the free edge, the conventional local strength-of-materials criterion is always satisfied. This criterion for the brittle or quasi-brittle materials, applicable in situations without stress singularity or existing crack, can be written as:

$$\sigma \geq S. \tag{1}$$

It states that for a structure to fracture, the stress σ must be equal to or exceed the corresponding strength of the material S.

On the other hand, Linear Elastic Fracture Mechanics (LEFM) relies on the existence of a crack to be applicable, making it inappropriate for structures that are free of cracks. Fracture mechanics Griffith's [40] energy criterion is formulated for situations involving large cracks:

$$G \geq G_c, \tag{2}$$

asserts that failure occurs when the energy release rate G, representing the driving force of the crack, equals or exceeds the material fracture toughness G_c.

When the stress-based criterion (Eq.(1)) is applied to situations involving singularities, the condition is invariably satisfied for any given applied stress. Conversely, when a crack is absent then the fracture mechanics criterion (Eq.(2)) is never satisfied as the ERR is zero. This presents a paradox: while the former criterion dictates that fracture occurs near the singularity at whatever the applied load, the latter implies that failure never occurs. Consequently, both criteria yield contradictory predictions in situations involving singularities. Moreover, experimental evidence (see Refs. [41–43]) indicates that fracture initiation does indeed occur in the singularity region under finite loads, making both criteria invalid for cases, such as laminates with free edge effects, where singularities exist.

As a result, both fracture criteria are considered inadequate for addressing the delamination due to free edge effects. Nevertheless, there are effective non-local methods available to predict free edge delamination. These methods are either stress or energy-based, depend on an empirical characteristic length and are summarised by Taylor [44] as Theory of Critical Distances (TCD). To remove the dependency on this unknown length parameter, Leguillon [45] in the framework of Finite Fracture Mechanics (FFM), proposed a coupled stress-energy fracture criterion. This FFM eliminates the requirement of prior assessment of the characteristic length, relying solely on intrinsic material properties such as strength and fracture toughness. Although FFM is a relatively newer criterion, having been introduced just two decades ago, its scope continues to expand.

Although several comprehensive review papers address the free edge effect in composite materials, as outlined in the preceding section, this paper specifically focuses on the delamination due to the free edge effect. Unlike previous works, this concise review critically examines the TCD and FFM approaches in addressing free edge delamination, offering an in-depth comparison of their strengths and limitations. The primary objective of this paper is to offer a systematic review that guides researchers in selecting appropriate methodologies for modelling and predicting free edge delamination, particularly aiding those less familiar with the details of these approaches.

The paper is organised as follows: Section 2 introduces the TCD framework, where stress- and energy-based methods are discussed in the context of free edge delamination. Section 3 provides a detailed overview of the FFM approach, exploring its relevance to free edge delamination problem. In Section 4, related models such as Cohesive Zone Models (CZM) and Phase-Field Models (PFM) are briefly discussed, particularly their applicability to crack initiation near singularities. Finally, Section 5 presents a summary of the key conclusions derived from the critical analysis of the discussed methods.

2. Theory of Critical Distances

Theory of Critical Distances (TCD) is the name given by Taylor [44] to the group of theories that predict material failure in the presence of high-stress concentrations. These theories share common features: they are all continuum mechanics-based approaches, assume linear elastic material behaviour, and incorporate the characteristic length, which is considered a material property, known as the critical distance. In the following sections, TCD methods are discussed in detail. Among them, two methods are modifications of strength-of-materials-based criteria, while two are developments of fracture mechanics-based criteria.

2.1. Point Method and Line Method

The Point Method (PM) states that failure occurs if stress at a critical distance (c_o) from high-stress gradient point equals the strength of the material. It is the simplest manifestation of TCD and is illustrated in Fig. 5(a). Mathematically it can be written as:

$$\sigma_{iz}(y) \geq S_i \quad \forall \quad y \in \Omega_c \qquad i \in \{x, y, z\}, \tag{3}$$

where σ_{iz} is interlaminar stress component of the laminate with free edge effects, S_i is corresponding interface strength, and Ω_c is the set of all points on the potential crack $\Omega_c(c_o)$. The PM requires the overloading of crack prior to the crack initiation.

According to the Line Method (LM), failure occurs when the average stress within a certain distance from a singularity point equals or exceeds the corresponding strength:

$$\frac{1}{d_o}\int_0^{d_o} \sigma_{iz}(y)\, dy = \overline{\sigma}_{iz} \geq S_i, \tag{4}$$

where $\overline{\sigma}_{iz}$ represents the average interlaminar stress component, and d_o is the critical distance (see Fig. 5(b)), that represents the material interface characteristic.

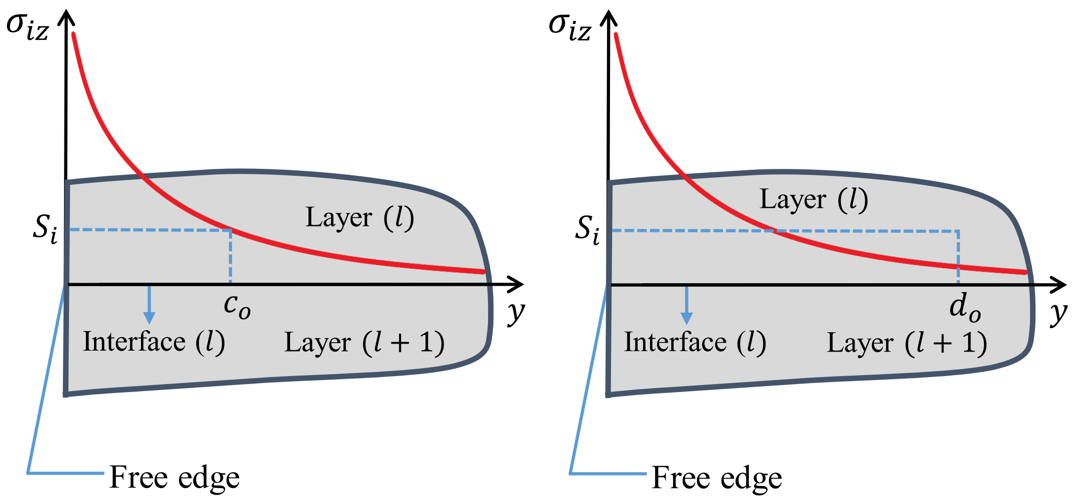

(a) (b)

Fig. 5. Critical distance in (a) Point Method (PM) and (b) Line Method (LM).

The first among TCD methods to be introduced is LM by Neuber [46] in 1958, followed by PM, proposed by Peterson [47] in 1959. Both PM and LM are developed as a part of investigations into fatigue failure in metallic components containing notches. In 1974, Whitney and Nuismer [48] independently introduced PM and LM for predicting the uniaxial tensile static strength of laminated composites containing notches, unaware of Neuber's and Peterson's earlier work. Drawing inspiration from Whitney and Nuismer, Kim and Soni [49] first implemented LM for predicting delamination initiation in composite laminates with free edges. Initially, Kim and Soni [49] applied LM only to the interlaminar normal stress distribution at the free edge. To take into account all three interlaminar stresses, they later introduced a criterion of the form [50]:

$$\left(\frac{\overline{\sigma}_{xz}}{S_x}\right)^2 + \left(\frac{\overline{\sigma}_{yz}}{S_y}\right)^2 + \left(\frac{\overline{\sigma}_{zz}{}^2}{S_z\, S_z^c}\right) + \overline{\sigma}_{zz}\left(\frac{1}{S_z} - \frac{1}{S_z^c}\right) \geq 1, \tag{5}$$

where S_x and S_y represent the interlaminar shear strengths for σ_{xz} and σ_{yz}, respectively, S_z is the tensile interlaminar normal strength for σ_{zz}, and S_z^c is compressive strength. Notably, $\overline{\sigma}_{zz}$ takes compression of the interface into consideration and assumes that it can delay the delamination.

Brewer and Lagace [51] on the other hand, squared the interlaminar normal stress and assumed that the influence of compressive stress is insignificant compared to the quadratic terms and hence does not delay delamination:

$$\left(\frac{\overline{\sigma}_{xz}}{S_x}\right)^2 + \left(\frac{\overline{\sigma}_{yz}}{S_y}\right)^2 + \left(\frac{\overline{\sigma}_{zz}}{S_z}\right)^2 + \left(\frac{\overline{\sigma}_{zz}}{S_z^c}\right)^2 \geq 1. \tag{6}$$

In Ye's [52] fracture criterion, the interlaminar normal compressive stress is not considered. Therefore, the criterion is written as:

$$\left(\frac{\overline{\sigma}_{xz}}{S_x}\right)^2 + \left(\frac{\overline{\sigma}_{yz}}{S_y}\right)^2 + \left(\frac{\langle\overline{\sigma}_{zz}\rangle}{S_z}\right)^2 \geq 1, \tag{7}$$

where, by using MacAuley bracket, $\langle\overline{\sigma}_{zz}\rangle$ is be defined as:

$$\langle\bar{\sigma}_{zz}\rangle = \begin{cases} 0, & \bar{\sigma}_{zz} < 0 \\ \bar{\sigma}_{zz}, & \bar{\sigma}_{zz} \geq 0. \end{cases} \tag{8}$$

Furthermore, in the model discussed by Marion [53] the interlaminar compressive strength S_z^c is considered to be significantly greater (infinite) than the tensile strength S_z, causing the quadratic term related to $\overline{\sigma}_{zz}$ to vanish. Nevertheless, the delay in delamination due to interlaminar compressive stress is considered. The interaction of the interlaminar stress components is expressed as:

$$\left(\frac{\overline{\sigma}_{xz}}{S_x}\right)^2 + \left(\frac{\overline{\sigma}_{yz}}{S_y}\right)^2 + \frac{\overline{\sigma}_{zz}}{S_z} \geq 1. \tag{9}$$

Interestingly, in implementing the various LM versions (considering single or all three interlaminar stress components) discussed above for predicting free edge delamination, researchers have employed different approaches to determine the material interface characteristic critical distance d_0. For instance, Kim and Soni [49], Ye [52], and Sun and Zhou [54] related this characteristic/critical length with the order of ply thickness. While Kim and Soni [49] define it to be equal to a single ply thickness, Ye [52] and Sun and Zhou [54] set it equal two ply thicknesses. Brewer and Lagace [51] recommended determining it from experimental results (edge delamination). Additionally, others such as Lagunegrand et al. [42] and Lorriot et al. [41] have also suggested experimental determination.

2.2. Imaginary Crack Method and Finite Crack Extension

The Imaginary Crack Method (ICM) is a fracture mechanics approach that assumes an inherent and imaginary flaw at the singularity. The ICM predicts the failure when the stress intensity factor (SIF) or equivalently energy release rate (ERR) at this imaginary crack becomes equal to the fracture toughness.

In the context of free edge delamination initiation, O'Brien [55] pioneered a method that determines the onset of delamination load which has an implicit assumption of crack present at the interface that triggers delamination. O'Brien derived an elegant expression for determination of ERR (G) that is independent of the delamination size:

$$G = \frac{\varepsilon^2 t}{2}(E_{LAM} - E^*), \tag{10}$$

where ε is nominal strain and t is laminate thickness. E_{LAM} is axial stiffness (tangent modulus) of a symmetric uncracked laminate and is calculated from laminate theory:

$$E_{LAM} = \frac{1}{tX_{11}}, \tag{11}$$

where X_{11} is the first element of the inverse extensional stiffness matrix $A_{ij}^{-1}(i, j = 1,2,3)$. E^* is the axial stiffness of completely delaminated (at one or multiple interfaces) laminate:

$$E^* = \frac{1}{t}\sum_{i=1}^{m} E_i t_i, \tag{12}$$

where m is the number of sublaminates formed by delamination (see Fig. 6), and E_i and t_i are the axial stiffness and thickness of the i^{th} sublaminate, respectively.

Furthermore, Eq.(10) can be utilised to determine the delamination onset strain ε_c, if the critical value of ERR G_c is known, using:

$$\varepsilon_c = \sqrt{\frac{2G_c}{t(E_{LAM} - E^*)}}. \tag{13}$$

In fact, O'Brien performed tension test of 11-ply $[(\pm 30)_2/90/\overline{90}]_s$ laminate to evaluate ε_c and utilised Eq.(10) to determine G_c for the onset of delamination. Subsequently, implementing this calculated G_c, O'Brien predicted the delamination onset strain of $[+45_n/-45_n/0_n/90_n]_s$ (n=1,2,3) laminates. O'Brien obtained good agreement between predictions and experimental test results.

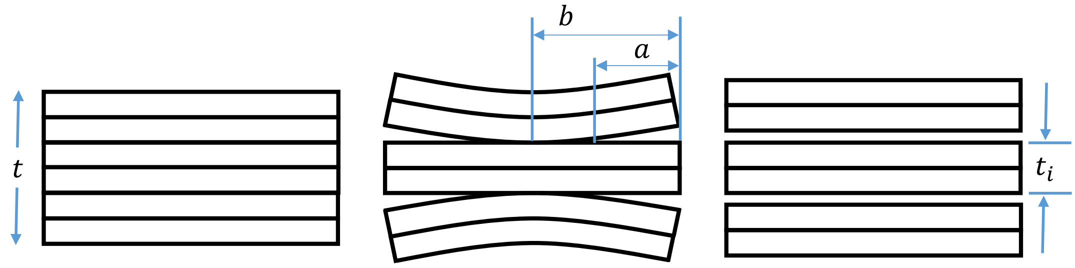

Fig. 6. Sublaminates formed due to free edge delamination.

While O'Brien's [55] expression (Eq.(10)), which is independent of crack size, may provide accurate predictions for delamination onset, it is important to note that it contradicts the fact that it is derived using an implicit assumption of inherent delamination.

There are other approaches in the context of free edge delamination that can be categorised under ICM. Among these approaches, Rybicki et al. [56] investigated and modelled the initiation and stable growth of the delamination at the free edge by employing finite element analysis (FEA) to an existing flaw length. It is discussed that there is a need to determine a characteristic length of a crack to be utilised in fracture mechanics computation for delamination initiation. Rybicki et al. used ply thickness as a characteristic length and obtained predictions of delamination initiation within 1.7% of the measured value. Wang and Crossman [57] further developed the fracture mechanics approach proposed by Rybicki et al. [56] to model free edge delamination and transverse cracking, formulating a theory in each case. The initiation and growth behaviour of crack is described by superposing the ERR and R-curve of the material. Leguillon [58] proposed an asymptotic process for cross-ply laminates at interfaces along free edges which considers the existence of micro-cracks or notches. The characteristic fracture length, which Leguillon termed as process zone, is estimated using interface fracture toughness. This length is found to be of the same order of magnitude as the characteristic inhomogeneity length, i.e., fibre diameter.

The other theory that falls under energy based TCD approaches is Finite Crack Extension (FCE). It is a modification to the conventional fracture mechanics which considers crack growth as a discontinuous process that occurs through finite extension Δa instead of infinitesimal extension da. This discontinuous crack growth is depicted in Fig. 7. FCE assumes the amount of crack extension Δa to be a material constant. This theory is essentially analogous to LM but applied to thermodynamic energy-based condition between two states of structure that captures the finite crack extension. Mathematically FCE is written as:

$$\frac{1}{\Delta a}\int_{0}^{\Delta a} G_j(a)\, da \geq G_{jc}, \quad j \in \{I, II, III\} \tag{14}$$

where j represents the different modes of fracture. The energy condition (Eq.(14)) can also be equivalently written in terms of SIF k and relating it with the critical value of SIF k_c:

$$\frac{1}{\Delta a}\int_{0}^{\Delta a} (k_j(a))^2\, da \geq k_{jc}^2. \tag{15}$$

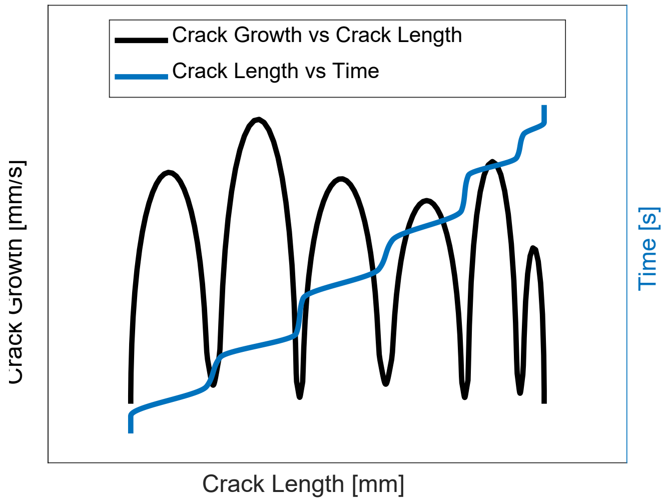

Fig. 7. Illustration of discontinuous crack growth through finite crack extension.

It is noted that the concept of crack propagation occurring in finite steps rather than continuously, as discussed in defining FCE, defines the framework of Finite Fracture Mechanics (FFM). However, the initialism 'FFM' is predominantly used in the literature to denote the coupled stress-energy criterion, which also falls within the FFM framework but lies outside of TCD. In fact, Eq.(14) or (15) is developed by Pugno and Ruoff [59] under the name of Quantized Fracture Mechanics (QFM) and by Taylor et al. [60] under the name Finite Fracture Mechanics (FFM). Therefore, to maintain consistency with existing literature and to avoid confusion, the initialism ‘FFM’ in this paper refers specifically to the coupled stress-energy criterion which is discussed in the following section.

3. Finite Fracture Mechanics

Hashin [61] introduced the Finite Fracture Mechanics (FFM) concept while analysing the development of multiple cracking in composites and demonstrated that the ERR of finite cracks can be utilised to a Griffth-like fracture condition. Nevertheless, the size of an unknown finite crack must be determined additionally besides unknown failure load.

TCD approaches whether stress or energy-based depend on an unknown empirical characteristic length. This length parameter, which varies based on the material and geometry of the structure, must be determined beforehand through relevant experiments. Therefore, to eliminate the issue with an unknown characteristic length that has unclear physical meaning, Leguillon [45] proposed a novel coupled stress-energy criterion in the FFM framework, drawing inspiration from the experimental observations of Parvizi et al. [62]. It supports the concept that, for fracture while stress and energy criteria are individually necessary, their combination provides a sufficient condition for it to occur. According to the FFM coupled criterion, a finite crack develops instantaneously upon initiation if both the stress and energy criteria are satisfied simultaneously:

$$\begin{cases} f\left(\dfrac{\sigma_{iz}(y)}{S_i}\right) \geq 1 \quad \forall \quad y \in \Omega_c(\Delta a) \\ \dfrac{1}{\Delta a}\displaystyle\int_0^{\Delta a} \dfrac{g\big(G_j(a)\big)}{G_c} da \geq 1 \end{cases} \quad i \in \{x, y, z\}, j \in \{I, II, III\}, \tag{16}$$

where G_c is a mixed-mode fracture toughness. Eq.(16) is a general form of FFM criterion that considers combining PM and FCE. Instead of utilising PM, Cornetti et al. [63] introduced a FFM coupled criterion that incorporates LM, whose general form can be written as:

$$\begin{cases} f\left(\dfrac{\overline{\sigma}_{iz}}{S_i}\right) \geq 1 \\ \dfrac{1}{\Delta a}\displaystyle\int_0^{\Delta a} \dfrac{g\big(G_j(a)\big)}{G_c} da \geq 1 \end{cases}. \tag{17}$$

In the most general case, the FFM system of equations (16) or (17) leads to solving an optimisation problem to find the minimum load that satisfies both stress and energy conditions for all considered crack configurations. This enables the prediction of both the size of an unknown finite crack and its corresponding failure load, provided that the material intrinsic properties such as strength and fracture toughness are known. Consequently, avoiding the requirement of a priori assessment of an unknown length parameter. The finite crack size in the FFM framework becomes the structural parameter that is no longer a material constant and is output to the FFM system ((16) or (17)), instead of being an input as in TCD. Furthermore, FFM generally provides improved solutions compared to TCD, especially when the structural size approaches or falls below the critical distance, where TCD breaks down.

Stress-based TCD approaches are difficult to understand as to why they are effective since these fracture criteria utilise elastic stress at a certain distance (PM) or averaged over a region (LM) and therefore lacking strong theoretical foundation. In contrast, FFM represents a physical mechanism and real behaviour of cracking phenomenon, which is discontinuous crack growth through finite crack extension. In fact, this discontinuous crack growth is observable in various materials, such as aluminium alloy [64], bone [65], and polymers [66], particularly during the initial stages of the cracking process. This makes FFM theoretically robust, providing realistic and valid predictions. Therefore, PM and LM are simply effective because they provide approximate predictions to FCE [67], which is a simplified form of FFM.

FFM incorporates the conventional strength-of-materials criterion as a limiting case, applicable when stress singularities are negligible, and fracture mechanics criterion as another limiting case, involving structures with strong singularities. Therefore, FFM bridges the gap between the two criteria and has far-reaching consequences. It has been implemented in various materials and structures across different scenarios, including both singular and non-singular stress concentrators, for predicting the initiation of cracks. Examples of these applications are V-notches [45,68,69], bolted joints [70], open-hole laminates [71–73], single-lap adhesive joints [74], solid oxide fuel cells under thermomechanical loading [75], and transverse cracking in cross-ply laminates [76]. In addition to defining the length and direction of a crack, as is the case with straight crack extension in 2D scenarios, initiation of a 3D crack poses a challenge due to the need to define an additional parameter, i.e., crack front, by using an infinite number of variables. The application of FFM models in 3D cases has been relatively limited. Following Leguillon's [77] extension of FFM to the prediction of 3D bimaterial interface corner crack by utilising 3D singularity theory and matched asymptotic expansions, García et al. [76] investigated the initiation of transverse cracks in cross-ply laminates using the 3D FFM. In the case of woven composites, Doitrand et al. [78] utilised it for the prediction of damage strain at initiation, which enabled the assessment of the configuration of a crack such as location, length, orientation, and decohesion length. To simplify the complexities related to actual crack shapes, both García et al. [76] and Doitrand et al. [78] used simplifying approximations for the shape of the crack, which prevented the determination of true crack shape. In contrast, Doitrand and Leguillon [79] reasonably predicted the onset of crack in aluminium-epoxy specimens under four-point bending by employing interface normal stress isocontours to determine the shape of the crack using a single parameter. Later on, they used this method to predict the initiation of cracks in scarf adhesive joints [80], using the crack surface area to parameterise the crack shape. Additionally, Yosibash and Mittelman [81] expanded the FFM into a 3D case for sharp V-notches under mixed-mode I/II/III loadings and validated their model through experimental tests. Moreover, Weißgraeber et al. [82] and Doitrand et al. [83] present thorough reviews that explore both the theoretical foundations of FFM and its practical application.

Some efforts have been made to implement FFM to address free edge delamination under remote tensile loads in layered structures, utilising a variety of techniques. Frey et al. [84] employed a closed-form analytical model based on the FFM criterion. Dölling et al. [85] combined FFM with the scaled boundary finite element method (SBFEM). Martin et al. [86] and Hebel et al. [87] used FEM to calculate energy and stresses. Under thermal loading, Dölling et al. [88] and Frey et al [89] predicted critical thermal loads of laminates exhibiting free edge effects. However, it is noted that all these aforementioned methods for addressing free edge delamination are based on the generalised plane strain condition. For this reason, Burhan et al. [90] recently implemented a 3D FFM criterion to predict free edge delamination in angle-ply laminates under remote tensile loading. By asserting the initiation of a semi-elliptically shaped crack from the free edge, it is demonstrated that accurate predictions can be obtained by hypothesising homothetic crack extension.

Fig. 8 compares the predictions of free edge delamination stress as a function of normalised effective ply thickness n for the AS1/3501-6 material system with a $[\pm 15_{\mathrm{n}}]_{\mathrm{s}}$ layup sequence, using various fracture criteria: 3D FFM (Burhan et al. [90]), 2D FFM (Dölling et al. [85]), and LM, ICM (Brewer and Lagace [51]). These predictions are compared against edge delamination experimental data Brewer and Lagace [51]. All criteria show close agreement with the experimental results, except LM, which is slightly conservative at lower n values. Notably, for LM predictions of free edge delamination, Brewer and Lagace [51] assessed parameters such as interlaminar strength and critical length values for three different layup sequences ($[\pm 15_{\mathrm{n}}]_{\mathrm{s}}$, $[\pm 15_{\mathrm{n}}/0_{\mathrm{n}}]_{\mathrm{s}}$, $[0_{\mathrm{n}}/\pm 15_{\mathrm{n}}]_{\mathrm{s}}$). Assessment of these parameters for a single layup sequence can yield more accurate LM predictions, as can be seen in the work of Lorriot et al. [41].

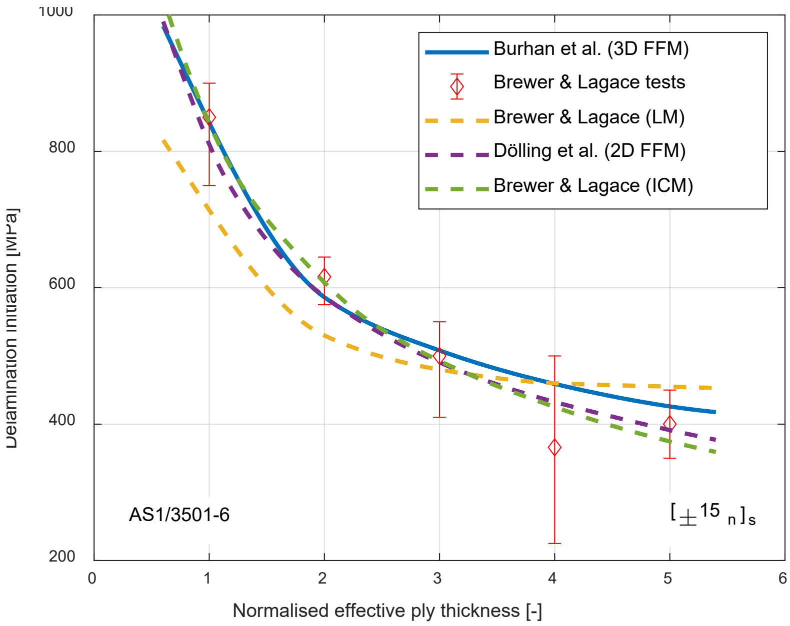

Fig. 8. Comparison of delamination initiation stress due to free edge effect as a function of normalised effective ply thickness for the AS1/3501-6 material system with $[\pm 15_n]_s$ layup sequence, using 3D FFM (Burhan et al. [90]), LM, ICM, and edge delamination experimental test data from Brewer and Lagace [51], and 2D FFM (Dölling et al. [85]).

4. Related fracture analysis theories

The most related models that can be implemented for crack initiation problems in the vicinity of high stress gradients are Cohesive Zone Models (CZM) and Phase-Field Models (PFM). Both are discussed briefly in the following sections.

4.1. Cohesive Zone Models

Cohesive Zone Models (CZM) are a model based on damage mechanics which considers the inelastic effects that occur in a fracture process zone can be lumped into a surface, modelled as a cohesive zone. The CZM approach goes back to Barenblatt [91] and Dugdale [92] models. The traction τ between the potential crack surfaces in this cohesive zone is related to the separation Δ through the constitutive traction-separation law $\tau(\Delta)$. The shape of this constitutive law has to be identified along a pre-defined path. In case of the bilinear law, as illustrated in Fig. 9 for a laminate with free edge effects, traction τ increases with respect to separation Δ within an initial elastic response until the material strength τ^o is reached before damage initiation. Penalty stiffness K is defined to ensure the potential crack surfaces are stiff within elastic response regime. The material strength τ^o and penalty stiffness defines the damage onset separation Δ^o. From this point, stiffness degradation occurs which is controlled by a damage variable d. The traction τ linearly decreases with increasing separation Δ

representing softening behaviour until the critical opening is achieved Δ^f. The irreversible bilinear constitutive law for the damage evolution can be defined as:

$$\tau(\Delta) = K(1-d)\Delta \qquad 0 \le d \le 1 \tag{18}$$

where value of d as 0 and 1 depicting damage onset and critical opening, respectively. CZM, similar to FFM, require two material parameters: material strength τ^o and fracture toughness G_c representing the amount of energy dissipated until the critical opening is achieved Δ^f. This G_c can be determined using separation work:

$$G_c = \int_0^{\Delta^f} \tau(\Delta)\, d\Delta. \tag{19}$$

The CZM implementation offers one of the alternative approaches to predict crack initiation and growth. In the context of free edge delamination, the work of Turon et al. [93] is worth mentioning, along with those of others [94,95] and a recent study [96].

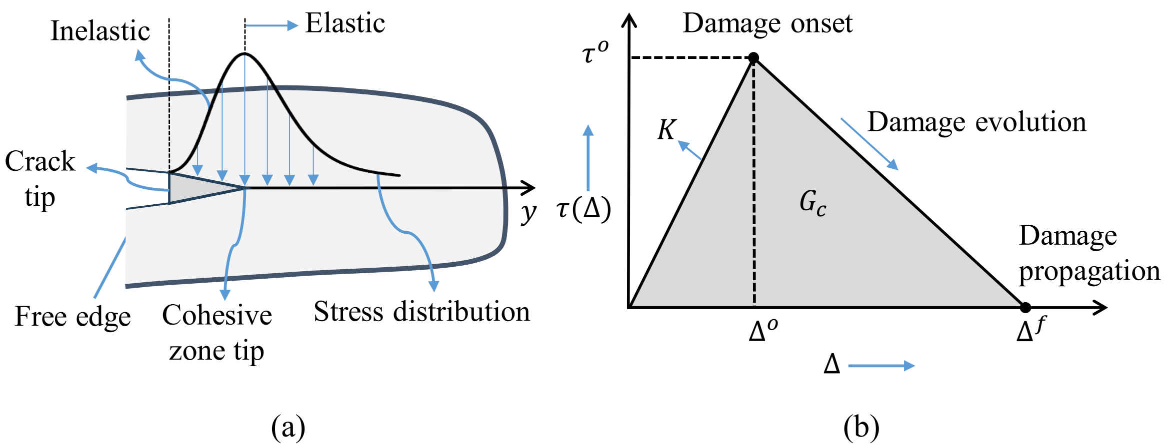

Fig. 9. Schematic illustration of (a) Cohesive Zone Model at the free edge and (b) its corresponding bilinear constitutive law.

Frey et al [89] predicted the critical thermal failure load $|\Delta T_f|$ due to free edge effect in the T800/914 material system using 2D FFM and compared these predictions with CZM, implemented as a secondary fracture criterion. Fig. 10 (a) illustrates the comparison with respect to normalised effective ply thickness n for a $[\pm 45_n]_s$ layup sequence, while Fig. 10 (b) shows the comparison with respect to ply orientation θ for a given n =16. The predictions of 2D FFM closely match those of CZM, although CZM results are more conservative, with a maximum relative error of 19%. This deviation can be mitigated by using LM as a stress criterion, as Frey et al [89] used PM, or by choosing the shape of the traction-separation law in CZM.

It is important to note that CZM, along with issues related to identifying traction-separation law, necessitates overcoming difficulties with convergence in the respective FEA due to being highly non-linear.

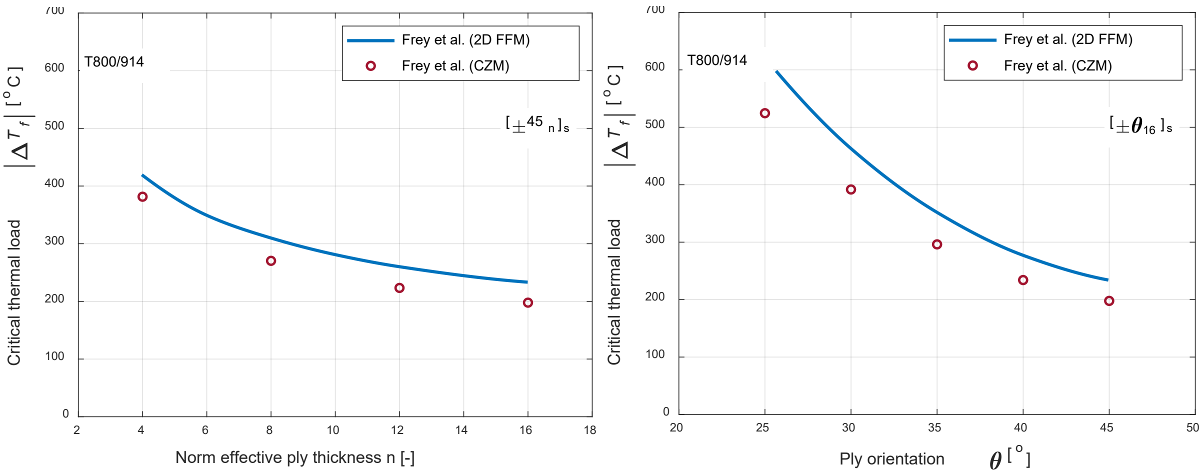

(a) (b)

Fig. 10. Comparison of thermal failure load $|\Delta T_f|$ of laminates exhibiting free edge effects, using 2D FFM and CZM for the T800/914 material system, with respect to (a) normalised effective ply thickness n and (b) ply orientation θ (Data from Frey et al [89]).

4.2. Phase-Field Models

Phase-Field Models (PFM) are based on a variational approach of brittle fracture that aims to determine the displacement field and a set of cracks simultaneously by minimising the total potential energy of the body. The linear elastic variational model is proposed by Francfort and Marigo [97] which quantified crack initiation as well as crack path. The numerical implementation of this fracture model is presented by Bourdin et al. [98] where cracks are approximated as smeared crack strips and to describe the damage state of a structure, a phase field variable $d \in [0,1]$ is introduced. For improving efficiency of the simulations, numerical implementation to obtain the solution of governing equations of PFM, which is of particular importance, is performed using FEM [99], peridynamics [100], and the meshless method [101]. FEM based implementation is the most commonly used and therefore numerous aspects of which are improved, such as computational efficiency [102] and numerical accuracy and stability [103,104].

5. Concluding remarks

The singular nature of interlaminar stresses at the free edge of a laminate makes both conventional strength-of-materials and fracture mechanics criteria unsuitable to implement. This paper discusses how these limitations led to the development of the Theory of Critical Distances (TCD), which introduces a critical distance—an experimentally determined material constant—to predict failure. TCD methods, whether stress- or energy-based, rely on this characteristic length which is an input to the fracture analysis in the model.

Finite Fracture Mechanics (FFM), in contrast, combines the non-local strength of materials and fracture mechanics criteria and assumes spontaneous finite crack initiation when both stress and energy conditions are met simultaneously. FFM yields both the failure load and the size of the finite crack without requiring a pre-determined length parameter. Instead, finite crack size is a structural parameter that depends on both geometry and material in FFM and is an output of the analysis in the model. Additionally, other models such as Cohesive Zone Models (CZM) and Phase-Field Models (PFM) are briefly discussed as alternatives for predicting failure initiation at stress singularities.

Moreover, the answer to the question of why TCD works lies in FFM. FCE, which is a simplified form of FFM, has a robust theoretical foundation, as it represents a physical mechanism of discontinuous crack growth through finite crack extension. Stress-based TCD theories are effective because they provide approximate predictions close to FFM. Furthermore, TCD has some drawbacks apart from an unknown length parameter whose physical meaning is not clear. It yields unreliable results, especially when the structural size falls below the critical distance. Although FFM overcomes this disadvantage, TCD can still be implemented in situations where structural size is significantly greater than the critical distance. In summary, based on the above-concluding remarks, FFM in its coupled form emerges as an advancement of TCD, representing a real behaviour of discontinuous cracking phenomenon unlike PM or LM, and does not require a priori determination of an unknown length parameter, a drawback inherent in all TCD methods.

CRediT authorship contribution statement

Mohammad Burhan: Conceptualisation, Methodology, Formal Analysis, Investigation, Writing-Original Draft, Visualisation. Zahur Ullah: Writing - review and editing, Supervision, Project Administration, Funding acquisition. Zafer Kazancı: Writing - review and editing. Giuseppe Catalanotti: Writing - review and editing, Supervision, Funding acquisition.

Declaration of competing interest

The authors declare that they have no known competing financial interests or personal relationships that could have appeared to influence the work reported in this paper.

Data availability

Data will be made available on request.

Acknowledgements

This study was conducted as part of the Belfast Maritime Consortium UKRI Strength in Places project, 'Decarbonisation of Maritime Transportation: A return to Commercial Sailing' led by Artemis Technologies, Project no. 107138.

References

[1] Böhm H, Richter J, Kim J, Joo G, Jang HK, Jeong M, et al. Glass-fiber mat/PA6 composite tubes subjected to dynamic axial crush loading—Experimental evaluation and high fidelity modeling of failure phenomena. Compos Struct 2023;319:117115. https://doi.org/10.1016/j.compstruct.2023.117115.

[2] Li Y, Liu Z, Shen J, Lee TH, Banu M, Hu SJ. Weld Quality Prediction in Ultrasonic Welding of Carbon Fiber Composite Based on an Ultrasonic Wave Transmission Model. J Manuf Sci Eng Trans ASME 2019;141:1–15. https://doi.org/10.1115/1.4043900.

[3] Li HCH, Herszberg I, Davis CE, Mouritz AP, Galea SC. Health monitoring of marine composite structural joints using fibre optic sensors. Compos Struct 2006;75:321–7. https://doi.org/10.1016/j.compstruct.2006.04.054.

[4] Guan C, Zhan L, Yang X, Dai G, Xiao Y. Significant effect of vibration treatment on microwave curing carbon fiber reinforced plastic. J Reinf Plast Compos 2020;39:373–83. https://doi.org/10.1177/0731684420909532.

[5] Bruggi M, Taliercio A. Topology optimization of the fiber-reinforcement retrofitting existing structures. Int J Solids Struct 2013;50:121–36. https://doi.org/10.1016/j.ijsolstr.2012.09.009.

[6] Reddy JN, Arciniega RA. Shear deformation plate and shell theories: From Stavsky to present. Mech Adv Mater Struct 2004;11:535–82. https://doi.org/10.1080/15376490490452777.

[7] Ferreira AJM. Analysis of composite plates using a layerwise theory and multiquadrics

discretization. Mech Adv Mater Struct 2005;12:99–112. https://doi.org/10.1080/15376490490493952.

[8] Hayashi T. Analytical Study of Interlaminar Shear Stresses in Laminated Composite Plate. Trans Jpn Soc Aeronaut Sp. Sci, 1967, p. 43–8.

[9] Mittelstedt C, Becker W, Kappel A, Kharghani N. Free-Edge Effects in Composite Laminates-A Review of Recent Developments 2005-2020. Appl Mech Rev 2022;74:1–18. https://doi.org/10.1115/1.4054145.

[10] Pagano NJ, Pipes RB. The Influence of Stacking Sequence on Laminate Strength. J Compos Mater 1971;5:50–7. https://doi.org/10.1007/978-94-017-2233-9_20.

[11] Pagano NJ, Pipes RB. Some observations on the interlaminar strength of composite laminates. Int J Mech Sci 1973;15. https://doi.org/10.1016/0020-7403(73)90099-4.

[12] Kassapoglou C, Lagace PA. Closed Form Solutions for the Interlaminar Stress Field in Angle-Ply and Cross-Ply Laminates. J Compos Mater 1987;21:292–308. https://doi.org/10.1177/002199838702100401.

[13] Wang SS, Choi I. Boundary-layer effects in composite laminates: Part 1 free-edge stress singularities. J Appl Mech Trans ASME 1982;49:541–8. https://doi.org/10.1115/1.3162514.

[14] Wang SS, Choi I. Boundary-Layer Effects in Composite Laminates-Part 2. J Appl Mech 1982;49:541–8.

[15] Mittelstedt C, Becker W. The Pipes-Pagano-problem revisited: Elastic fields in boundary layers of plane laminated specimens under combined thermomechanical load. Compos Struct 2007;80:373–95. https://doi.org/10.1016/j.compstruct.2006.05.018.

[16] Yao WA, Nie YZ, Xiao F. Analytical solutions to edge effect of composite laminates based on symplectic dual system. Appl Math Mech (English Ed 2011;32:1091–100. https://doi.org/10.1007/s10483-011-1483-7.

[17] Nosier A, Maleki M. Free-edge stresses in general composite laminates. Int J Mech Sci 2008;50:1435–47. https://doi.org/10.1016/j.ijmecsci.2008.09.002.

[18] Sarvestani HY, Sarvestani MY. Free-edge stress analysis of general composite

laminates under extension, torsion and bending. Appl Math Model 2012;36:1570–88. https://doi.org/10.1016/j.apm.2011.09.028.

[19] Yazdani Sarvestani H, Yazdani Sarvestani M. Interlaminar stress analysis of general composite laminates. Int J Mech Sci 2011;53:958–67. https://doi.org/10.1016/j.ijmecsci.2011.07.007.

[20] Tahani M, Nosier A. Accurate determination of interlaminar stresses in general cross-ply laminates. Mech Adv Mater Struct 2004;11:67–92. https://doi.org/10.1080/15376490490257657.

[21] Carrera E. Theories and finite elements for multilayered plates and shells: A unified compact formulation with numerical assessment and benchmarking. Arch Comput Methods Eng 2003;10:215–96. https://doi.org/10.1007/BF02736224.

[22] Wenzel C, D'Ottavio M, Polit O, Vidal P. Assessment of free-edge singularities in composite laminates using higher-order plate elements. Mech Adv Mater Struct 2016;23:948–59. https://doi.org/10.1080/15376494.2015.1121526.

[23] Pipes RB, Pagano NJ. Interlaminar Stresses in Composite Laminates Under Uniform Axial Extension. J Compos Mater 1970;4:538–48. https://doi.org/10.1177/002199837000400409.

[24] Islam MS, Prabhakar P. Modeling framework for free edge effects in laminates under thermo-mechanical loading. Compos Part B Eng 2017;116:89–98. https://doi.org/10.1016/j.compositesb.2017.01.072.

[25] Raju IS, Crews JH. Interlaminar stress singularities at a straight free edge in composite laminates. Comput Struct 1981;14:21–8.

[26] Burhan M, Scalici T, Ullah Z, Kazancı Z, Catalanotti G. Investigating factors influencing interlaminar stresses and energy release rates of semi-elliptical cracks at free edges. Eng Fract Mech 2024:110274.

[27] Ye L, Yang BX. Boundary Layer Approach To Interlaminar Stresses in Composite Laminates With Curved Edges. J Reinf Plast Compos 1988;7:179–98. https://doi.org/10.1177/073168448800700207.

[28] Ahmadi I. Interlaminar stress analysis in general thick composite cylinder subjected to nonuniform distributed radial pressure. Mech Adv Mater Struct 2017;24:773–88.

https://doi.org/10.1080/15376494.2016.1196782.

[29] Wang X, Cai W, Yu ZY. An analytic method for interlaminar stress in a laminated cylindrical shell. Mech Adv Mater Struct 2002;9:119–31. https://doi.org/10.1080/153764902753510507.

[30] Kappel A, Dillen S, Mittelstedt C. Hygrothermomechanical analysis of the free-edge stress fields in cylindrical cross-ply laminated shells. Mech Adv Mater Struct 2023;30:676–93. https://doi.org/10.1080/15376494.2021.2022256.

[31] Shim DJ, Lagacé PA. An analytical method for interlaminar stresses due to global effects of ply drop-offs. Mech Adv Mater Struct 2005;12:21–32. https://doi.org/10.1080/15376490490491927.

[32] Ding S, Tong JW, Shen M, Huo Y. Three-dimensional elastic-plastic analysis of the interlaminar stresses for the AS4/PEEK composite laminate with a circular hole. Mech Adv Mater Struct 2010;17:406–18. https://doi.org/10.1080/15376494.2010.483322.

[33] Wigger HM, Becker W. Closed-form analysis of the stress field at rectangular corners of reinforcement patches. Mech Adv Mater Struct 2008;15:104–16. https://doi.org/10.1080/15376490701810431.

[34] Ivanova J, Valeva V, Petrova T, Becker W. Interfacial debonding of a piezoelastic bi-material structure applicable for wind rotor blades. Mech Adv Mater Struct 2015;22:813–8. https://doi.org/10.1080/15376494.2013.864433.

[35] Wu ZJ, Han C. A strong solution for a generalized plane strain unsymmetrical piezoelectric bi-layer laminates. Mech Adv Mater Struct 2017;24:122–30. https://doi.org/10.1080/15376494.2015.1107671.

[36] Salamon NJ. An Assessment of the Interlaminar Stress Problem in Laminated Composites. J Compos Mater 1980;14:177–94. https://doi.org/10.1177/002199838001400114.

[37] Kant T, Swaminathan K. Estimation of transverse/interlaminar stresses in laminated composites - a selective review and survey of current developments. Compos Struct 2000;49:65–75. https://doi.org/10.1016/S0263-8223(99)00126-9.

[38] Mittelstedt C, Becker W. Free-edge effects in composite laminates. Appl Mech Rev 2007;60:217–45. https://doi.org/10.1115/1.2777169.

[39] Chen, Y; Wang, Y;Wang H. Research progress on interlaminar failure behavior of fibre metal laminates. Adv Polym Technol 2020.

[40] Griffith AA. The phenomena of rupture and flow in solids. Philos Trans R Soc London Ser A, Contain Pap a Math or Phys Character 1921;221:163–98. https://doi.org//10.1098/rsta.1921.0006.

[41] Lorriot T, Marion G, Harry R, Wargnier H. Onset of free-edge delamination in composite laminates under tensile loading. Compos Part B Eng 2003;34:459–71. https://doi.org/10.1016/S1359-8368(03)00016-7.

[42] Lagunegrand L, Lorriot T, Harry R, Wargnier H, Quenisset JM. Initiation of free-edge delamination in composite laminates. Compos Sci Technol 2006;66:1315–27. https://doi.org/10.1016/j.compscitech.2005.10.010.

[43] Burhan M, Ullah Z. Experimental and numerical investigation of fracture characteristics in hybrid steel/composite and monolithic angle-ply laminates. SSRN Prepr 2024. https://doi.org/10.2139/ssrn.4838504.

[44] Taylor D. The theory of critical distances. Eng Fract Mech 2008;75:1696–705. https://doi.org/10.1016/j.engfracmech.2007.04.007.

[45] Leguillon D. Strength or toughness? A criterion for crack onset at a notch. Eur J Mech A/Solids 2002;21:61–72. https://doi.org/10.1016/S0997-7538(01)01184-6.

[46] Neuber H. Theory of notch stresses : principles for exact calculation of strength with reference to structural form and material, 1958.

[47] Peterson R. Notch-sensitivity. G Sines J L Waisman, Eds, Met Fatigue, McGraw-Hill, New York, 1959:293–306.

[48] Whitney JM., Nuismer RJ. Stress Fracture Criteria for Laminated Composites Containing Stress Concentrations. J Compos Mater 1974;8:253–65.

[49] Kim RY, Soni SR. Experimental and Analytical Studies On the Onset of Delamination in Laminated Composites. J Compos Mater 1984;18:70–80. https://doi.org/10.1177/002199838401800106.

[50] Kim RY, Soni SR. Failure of composite laminates due to combined interlaminar normal and shear stresses. Compos 86 Recent Adv Japan United States 1986;86:341–

50.

[51] Brewer JC, Lagace PA. Quadratic Stress Criterion for Initiation of Delamination. J Compos Mater 1988;22:1141–55. https://doi.org/10.1177/002199838802201205.

[52] Lin Ye. Role of matrix resin in delamination onset and growth in composite laminates. Compos Sci Technol 1988;33:257–77. https://doi.org/10.1016/0266-3538(88)90043-7.

[53] Marion G. Etude expérimentale et théorique de l'amorçage du délaminage au bord libre de matériaux composites stratifiés. PhD Thesis. Université Bordeaux I, 2000.

[54] Sun CT, Zhou SG. Failure of Quasi-Isotropic Composite Laminates with Free Edges. J Reinf Plast Compos 1988;7:515–57. https://doi.org/10.1177/073168448800700602.

[55] O'Brien TK. Characterization of Delamination Onset and Growth in a Composite Laminate. Damage Compos Mater ASTM STP 775, KL Reifsnider, E.d, Am Soc Test Mater 1982:140–67. https://doi.org/10.1520/STP34325S.

[56] Rybicki EF, Schmueser DW, Fox J. An Energy Release Rate Approach For Stable Crack Growth in the Free-Edge Delamination Problem. J Compos Mater 1977;11:470–87.

[57] Wang A, Crossman FW. Initiation and Growth of Transverse Cracks and Edge Delamination in Composite Laminates Part 1. An Energy Method. J Compos Mater 1980;14:71–87.

[58] Leguillon D. A method based on singularity theory to predict edge delamination of laminates. Int J Fract 1999;100:105–20.

[59] Pugno NM, Ruoff RS. Quantized fracture mechanics. Philos Mag 2004;84:2829–45. https://doi.org/10.1080/14786430412331280382.

[60] Taylor D, Cornetti P, Pugno N. The fracture mechanics of finite crack extension. Eng Fract Mech 2005;72:1021–38. https://doi.org/10.1016/j.engfracmech.2004.07.001.

[61] Hashin Z. Finite thermoelastic fracture criterion with application to laminate cracking analysis. J Mech Phys Solids 1996;44:1129–45. https://doi.org/10.1016/0022-5096(95)00080-1.

[62] Parvizi A, Garrett KW, Bailey JE. Constrained cracking in glass fibre-reinforced epoxy cross-ply laminates. J Mater Sci 1978;13:195–201.

https://doi.org/10.1007/BF00739291.

[63] Cornetti P, Pugno N, Carpinteri A, Taylor D. Finite fracture mechanics: A coupled stress and energy failure criterion. Eng Fract Mech 2006;73:2021–33. https://doi.org/10.1016/j.engfracmech.2006.03.010.

[64] Blom, A Hedlund, A Zhao, W Fathulla, A Weiss, B. Stickler, R. Short fatigue crack growth behaviour in Al2024 and Al7475. In: Miller KJ, delosRios ER, editors. The behaviour of short fatigue cracks (EGFI). London: MEP; 1986:37–66.

[65] Hazenberg JG, Taylor D, Lee TC. Mechanisms of short crack growth at constant stress in bone. Biomaterials 2006;27:2114–22. https://doi.org/10.1016/j.biomaterials.2005.09.039.

[66] Kinloch AJ, Shaw SJ, Tod DA, Hunston DL. Deformation and fracture behaviour of a rubber-toughened epoxy: 1. Microstructure and fracture studies. Polymer (Guildf) 1983;24:1341–54. https://doi.org/10.1016/0032-3861(83)90070-8.

[67] Taylor D. The theory of critical distances: a new perspective in fracture mechanics. Oxford, UK: Elsevier; 2007.

[68] Carpinteri A, Cornetti P, Pugno N, Sapora A, Taylor D. A finite fracture mechanics approach to structures with sharp V-notches. Eng Fract Mech 2008;75:1736–52. https://doi.org/10.1016/j.engfracmech.2007.04.010.

[69] Sapora A, Cornetti P, Carpinteri A. A Finite Fracture Mechanics approach to V-notched elements subjected to mixed-mode loading. Eng Fract Mech 2013;97:216–26. https://doi.org/10.1016/j.engfracmech.2012.11.006.

[70] Catalanotti G, Camanho PP. A semi-analytical method to predict net-tension failure of mechanically fastened joints in composite laminates. Compos Sci Technol 2013;76:69–76. https://doi.org/10.1016/j.compscitech.2012.12.009.

[71] Weißgraeber P, Felger J, Geipel D, Becker W. Cracks at elliptical holes: Stress intensity factor and Finite Fracture Mechanics solution. Eur J Mech A/Solids 2016;55:192–8. https://doi.org/10.1016/j.euromechsol.2015.09.002.

[72] Camanho PP, Erçin GH, Catalanotti G, Mahdi S, Linde P. A finite fracture mechanics model for the prediction of the open-hole strength of composite laminates. Compos Part A Appl Sci Manuf 2012;43:1219–25.

https://doi.org/10.1016/j.compositesa.2012.03.004.

[73] Martin E, Leguillon D, Carrère N. A coupled strength and toughness criterion for the prediction of the open hole tensile strength of a composite plate. Int J Solids Struct 2012;49:3915–22. https://doi.org/10.1016/j.ijsolstr.2012.08.020.

[74] Talmon l'Armée A, Becker W. Coupled stress and energy criterion for composite failure: Pointwise versus averaged evaluation of the stress criterion. Mech Adv Mater Struct 2020;27:1571–82. https://doi.org/10.1080/15376494.2018.1519618.

[75] Hebel J, Becker W. Numerical analysis of brittle crack initiation at stress concentrations in composites. Mech Adv Mater Struct 2008;15:410–20. https://doi.org/10.1080/15376490802135266.

[76] García IG, Carter BJ, Ingraffea AR, Mantič V. A numerical study of transverse cracking in cross-ply laminates by 3D finite fracture mechanics. Compos Part B Eng 2016;95:475–87. https://doi.org/10.1016/j.compositesb.2016.03.023.

[77] Leguillon D. An attempt to extend the 2D coupled criterion for crack nucleation in brittle materials to the 3D case. Theor Appl Fract Mech 2014;74:7–17. https://doi.org/10.1016/j.tafmec.2014.05.004.

[78] Doitrand A, Fagiano C, Carrère N, Chiaruttini V, Hirsekorn M. Damage onset modeling in woven composites based on a coupled stress and energy criterion. Eng Fract Mech 2017;169:189–200. https://doi.org/10.1016/j.engfracmech.2016.11.021.

[79] Doitrand A, Leguillon D. 3D application of the coupled criterion to crack initiation prediction in epoxy/aluminum specimens under four point bending. Int J Solids Struct 2018;143:175–82. https://doi.org/10.1016/j.ijsolstr.2018.03.005.

[80] Doitrand A, Leguillon D. Comparison between 2D and 3D applications of the coupled criterion to crack initiation prediction in scarf adhesive joints. Int J Adhes Adhes 2018;85:69–76. https://doi.org/10.1016/j.ijadhadh.2018.05.022.

[81] Yosibash Z, Mittelman B. A 3-D failure initiation criterion from a sharp V-notch edge in elastic brittle structures. Eur J Mech A/Solids 2016;60:70–94. https://doi.org/10.1016/j.euromechsol.2016.06.003.

[82] Weißgraeber P, Leguillon D, Becker W. A review of Finite Fracture Mechanics: crack initiation at singular and non-singular stress raisers. Arch Appl Mech 2016;86:375–

401. https://doi.org/10.1007/s00419-015-1091-7.

[83] Doitrand A, Duminy T, Girard H, Chen X. A review of the coupled criterion. Hal-04023438 2023.

[84] Frey C, Dölling S, Becker W. Closed-form analysis of interlaminar crack initiation in angle-ply laminates. Compos Struct 2021;257:113060. https://doi.org/10.1016/j.compstruct.2020.113060.

[85] Dölling S, Hahn J, Felger J, Bremm S, Becker W. A scaled boundary finite element method model for interlaminar failure in composite laminates. Compos Struct 2020;241:111865. https://doi.org/10.1016/j.compstruct.2020.111865.

[86] Martin E, Leguillon D, Carrère N. A twofold strength and toughness criterion for the onset of free-edge shear delamination in angle-ply laminates. Int J Solids Struct 2010;47:1297–305. https://doi.org/10.1016/j.ijsolstr.2010.01.018.

[87] Hebel J, Dieringer R, Becker W. Modelling brittle crack formation at geometrical and material discontinuities using a finite fracture mechanics approach. Eng Fract Mech 2010;77:3558–72. https://doi.org/10.1016/j.engfracmech.2010.07.005.

[88] Dölling S, Bremm S, Kohlstetter A, Felger J, Becker W. Predicting thermally induced edge-crack initiation using finite fracture mechanics. Eng Fract Mech 2021;252:107808. https://doi.org/10.1016/j.engfracmech.2021.107808.

[89] Frey C, Dölling S, Leštáková M, Becker W. Free-edge crack onset induced by thermal loading. Int J Solids Struct 2021;230–231:111160. https://doi.org/10.1016/j.ijsolstr.2021.111160.

[90] Burhan M, Scalici T, Ullah Z, Kazancı Z, Catalanotti G. A three-dimensional Finite Fracture Mechanics model to predict free edge delamination in angle ply laminates. Eng Fract Mech 2024;306:110156. https://doi.org/10.1016/j.engfracmech.2024.110156.

[91] Barenblatt GI. The Mathematical Theory of Equilibrium Cracks in Brittle Fracture. Adv Appl Mech 1962;7:55–129.

[92] Dugdale D. Yielding of steel sheets containing slits. J Mech Phys Solids 1960;8:100–4. https://doi.org/10.12989/cac.2015.15.5.735.

[93] Turon A, Dávila CG, Camanho PP, Costa J. An engineering solution for mesh size effects in the simulation of delamination using cohesive zone models. Eng Fract Mech 2007;74:1665–82. https://doi.org/10.1016/j.engfracmech.2006.08.025.

[94] Yang Q, Cox B. Cohesive models for damage evolution in laminated composites. Int J Fract 2005;133:107–37. https://doi.org/10.1007/s10704-005-4729-6.

[95] Mohammadi B, Salimi-Majd D. Investigation of delamination and damage due to free edge effects in composite laminates using cohesive interface elements. Eng Solid Mech 2014;2:101–18. https://doi.org/10.5267/j.esm.2014.2.001.

[96] Lu X, Ridha M, Chen BY, Tan VBC, Tay TE. On cohesive element parameters and delamination modelling. Eng Fract Mech 2019;206:278–96. https://doi.org/10.1016/j.engfracmech.2018.12.009.

[97] Francfort GA, Marigo JJ. Revisiting brittle fracture as an energy minimization problem. J Mech Phys Solids 1998;46:1319–42. https://doi.org/10.1016/S0022-5096(98)00034-9.

[98] Bourdin B, Francfort GA, Marigo JJ. Numerical experiments in revisited brittle fracture. J Mech Phys Solids 2000;48:797–826. https://doi.org/10.1016/S0022-5096(99)00028-9.

[99] Molnár G, Gravouil A. 2D and 3D Abaqus implementation of a robust staggered phase-field solution for modeling brittle fracture. Finite Elem Anal Des 2017;130:27–38. https://doi.org/10.1016/j.finel.2017.03.002.

[100] Roy P, Pathrikar A, Deepu SP, Roy D. Peridynamics damage model through phase field theory. Int J Mech Sci 2017;128–129:181–93. https://doi.org/10.1016/j.ijmecsci.2017.04.016.

[101] Amiri F, Millán D, Arroyo M, Silani M, Rabczuk T. Fourth order phase-field model for local max-ent approximants applied to crack propagation. Comput Methods Appl Mech Eng 2016;312:254–75. https://doi.org/10.1016/j.cma.2016.02.011.

[102] Heister T, Wheeler MF, Wick T. A primal-dual active set method and predictor-corrector mesh adaptivity for computing fracture propagation using a phase-field approach. Comput Methods Appl Mech Eng 2015;290:466–95. https://doi.org/10.1016/j.cma.2015.03.009.

[103] Singh N, Verhoosel C V., De Borst R, Van Brummelen EH. A fracture-controlled path-following technique for phase-field modeling of brittle fracture. Finite Elem Anal Des 2016;113:14–29. https://doi.org/10.1016/j.finel.2015.12.005.

[104] Wu JY. Robust numerical implementation of non-standard phase-field damage models for failure in solids. Comput Methods Appl Mech Eng 2018;340:767–97. https://doi.org/10.1016/j.cma.2018.06.007.